

Effect of spatial heterogeneity of porosity on gas transport in compacted MX-80 bentonite

Laura Gonzalez-Blanco¹, Enrique Romero^{2*} & Paul Marschall³

¹ International Centre of Numerical Methods in Engineering (CIMNE), Barcelona, Spain

² Universitat Politècnica de Catalunya (UPC), Barcelona, Spain

³ Nationale Genossenschaft für die Lagerung radioaktiver Abfälle (NAGRA), Wetingen, Switzerland

* enrique.romero-morales@upc.edu

Introduction

Understanding gas migration in compacted bentonite is of great importance for the assessment of the long-term safety of an HLW/SF repository. Gas transport in these clay-rich materials is affected by the soil state, in which the global dry density, the pore size distribution and its connectivity, the saturation state, the stress state and the heterogeneous distribution of porosity, may play important roles. Particularly, the present study aims at investigating, both experimentally and numerically, how the heterogeneity of compacted samples may influence the initiation and the propagation of preferential pathways following the lower dry density (clay gel) zones between coarse clay aggregates.

Material and stress paths followed

An experimental program was launched to perform tests on statically compacted MX-80 bentonite samples (dry density of 1.55 Mg/m³, porosity $\phi=0.446$ and water content 20%) with large-size aggregates (up to 4.5-9.5 mm). Main focus was given to investigate sample microstructure through micro-computed tomography (μ -CT) technique at different states of the sample: compacted, saturated and after a gas injection and dissipation test. A high-pressure oedometer cell was used to perform the saturation and gas injection tests (sample diameter of 50 mm and 20 mm high). The stress paths included three stages: (a) loading at constant water content to the compaction preconsolidation stress (~ 5 MPa); (b) saturation at constant vertical stress (~ 5 MPa); and (c) gas injection / dissipation test at constant vertical stress (~ 5 MPa). Gas (air and Helium) was injected at the bottom boundary using a volumetric rate of 2 mL/min up to a maximum gas pressure of 4 MPa (higher than the expected air-entry value of the compacted bentonite). Gas dissipation was then allowed at closed injection line and forcing the gas to flow upwards. Samples after the saturation and the gas injection / dissipation stages were unloaded at water undrained conditions for the microstructural analyses.

Results

The examination of the evolution of axial strain during the gas injection / dissipation stage revealed different deformation stages that have impact on gas migration issues. During the gas injection stage, the sample underwent a small expansion. After shut-off, expansion continued as a consequence of the gas pressure front propagation into the sample, which induced the pore fluid pressures (gas and liquid) to increase and the effective stress to decrease. Maximum expansion of the sample was usually associated with the breakthrough process, in which increasing outflow volumes were recorded. During the dissipation stage the pore fluid pressures decreased, inducing sample compression (Romero & Gonzalez-Blanco 2017, 2018).

Fig. 1 shows μ -CT images of samples at the different states previously described. As observed in the figure, the compacted state displayed a grain structure that is easily distinguishable. After saturation, the sample showed a more homogeneous structure although some boundaries between the original grains are still present (the original grain structure and weak grain boundaries did not completely vanish during the saturation process). It appeared that the gas injection process reactivated these low-density boundaries (clay gel and pores) by inducing some opening and desaturation of the gas pathways. These results were fundamental for a correct understanding and simulation of the coupled hydro-mechanical processes occurring during gas migration through a medium with local heterogeneity (random variation of porosity affecting intrinsic permeability and gas-entry value).

The correlation between CT gray value and dry density (calibrated with standardizing materials: aluminum, distilled water, and air) allowed reconstructing the local distribution of the initial dry density of the saturated sample (representative of the state before gas injection). The dry density typically ranged between 1.37 and 1.57 Mg/m³. Initial heterogeneity was then implemented in the modelling approach by a random distribution of four initial representative porosities (20% of elements with porosity $\phi=0.438$, 40% with $\phi=0.462$, 20% with $\phi=0.470$,

and 20% with $\phi=0.512$). Finite element Code_Bright was used for the 3D coupled hydro-mechanical simulations (Romero & Gonzalez-Blanco 2018). Fig. 2 presents the spatial distribution of porosity, gas absolute pressure, gas advective fluxes and degree of saturation at three different stages of the gas test (injection, shut-off and dissipation). The results clearly show that gas migration initiated and propagated due to the desaturation of paths in areas with low density material.

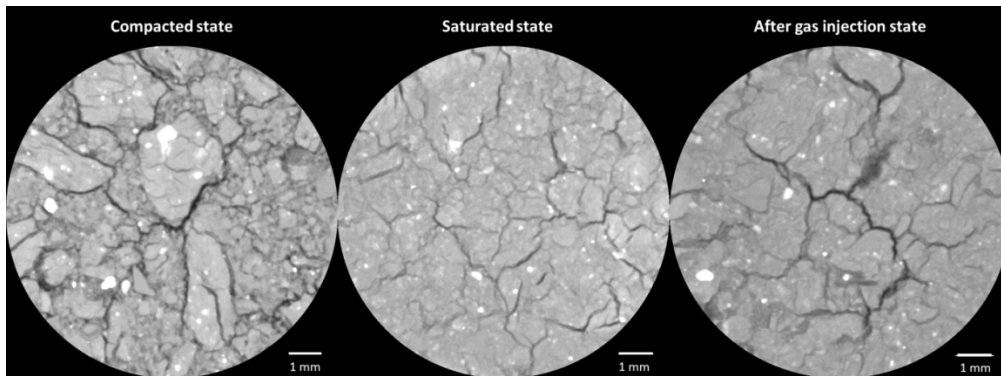


Fig. 1: μ -CT images of samples at compacted, saturated and after gas injection states.

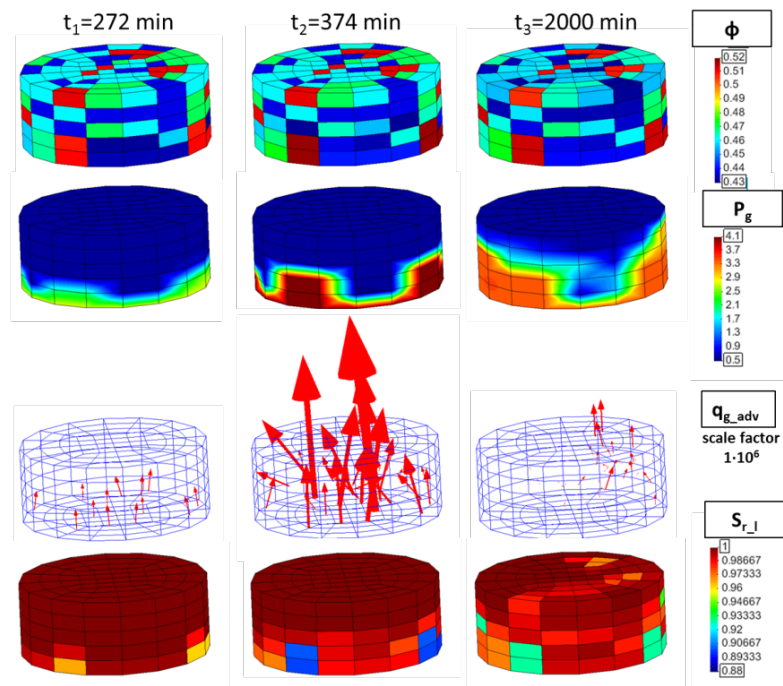


Fig 2: Spatial distribution of porosity (ϕ); b) absolute gas pressure (P_g in MPa); advective gas flow vectors (q_{g_adv}); and liquid degree of saturation ($S_{r,l}$) during the gas injection ($t_1=272$ min), at shut-off ($t_2=374$ min) and during the dissipation stages ($t_3=2000$ min).

Acknowledgements

Financial support of NAGRA (Switzerland) through different collaboration agreements with CIMNE (Spain) is greatly acknowledged.

References

- Romero, E. and Gonzalez-blanco, L. (2018) 'Hydromechanical processes associated with gas transport in Wyoming granular bentonite - Complementary laboratory experiments carried out at UPC in 12017', *Arbeitsbericht NAB 18-09*, p. 45
- Romero, E. and Gonzalez-Blanco, L. (2017) 'Hydro-mechanical processes associated with gas transport in MX-80 bentonite in the context of Nagra's RD&D programme', *Arbeitsbericht NAB 17-09*, p. 62.